# Modeling Biomaterials to Second Order

Lev Gruber and Charlie Schofield

December 14, 2024

**Abstract**

We create a non-linear correction term to Hooke's Law for polymeric materials. We proceed to simulate a simplified biological system by putting these massless, non-linear springs in series, between these springs we include masses that represent joints. Finally, we evaluate non-analytically solvable equations of motion to see how chaotic behavior arises as we vary spring constants, masses, and initial conditions.

## 1 Introduction

In Hooke's Law, the restorative force of a spring is proportional to its displacement. The proportionality is determined by the material properties of your spring. In the context of biological materials, structures are often created from repeated microscopic units leading to interesting macroscopic properties. Such materials are called polymeric materials. Unlike classical springs, these polymeric materials have three qualitatively different regimes under tension. For small displacements, the polymers are tightly balled and the main restorative force comes from untangling and entropic forces. For intermediate displacements we see compliance, the material yields and is easier to stretch as the effects of it being tightly wound diminish. In the large displacement regime, the limiting factor becomes how much you can stretch the individual monomers. The material becomes stiffer and can eventually break. These three regimes happen at different strains for different materials, since the underlying processes depend on the bond chemistry. Example stress/strain curves for Glass, Hair, and Skin are pictured in 1.

Our goal is to simulate the second and third regimes, that is the intermediate compliance and the growing stiffness in the large strain limit. Accounting for all three regimes can be done with more complicated models (see the Mooney-Rivlin solid), but this is a naive first step in that direction. We attempt to simulate these materials with the following generalized form:

$$\sigma = -k\epsilon - c\epsilon^2 \tag{1}$$

For some cross-sectional surface area $A$ and equilibrium length of our spring $L$, we can use the definitions of stress $\sigma = \frac{F}{A}$ and strain $\epsilon = \frac{x}{L}$. Substituting in these expressions, we arrive at an equation relating force to displacement:

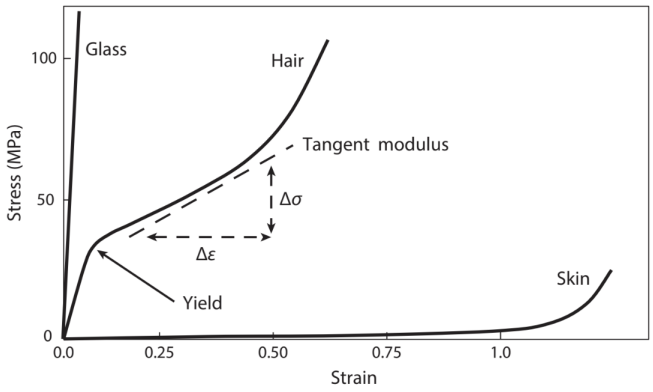


Figure 1: Different materials have different stress responses as a function of strain. These differences are shown for glass, hair, and skin. Note how skin doesn't experience the same initial stiffness due to the entropic forces associated with unraveling. These are the type of materials we will be analyzing. Image Credit: Gosline *Mechanical Design of Structural Materials in Animals*

$$F = A\left(-k\left(\frac{x}{L}\right) - c\left(\frac{x}{L}\right)^2\right) \tag{2}$$

Note that we chose $k$ and $c$ to be arbitrary constants with the appropriate units, so we can absorb the cross-sectional area into them:

$$F = -k\left(\frac{x}{L}\right) - c\left(\frac{x}{L}\right)^2 \tag{3}$$

# 2 The System

Our system is a classic setup of three coupled oscillators as seen in Figure 2. These springs have the same rest length, exactly a third the total length available. The difference between our setup and the canonical example is that these are non-linear oscillators, their force given by Eqn 3.

## 2.1 Lagrangian Derivation

Starting from our definition of the restorative force, we can use separation of variables to jump quickly to a potential for a generic spring with a quadratic force term.

$$U = \frac{k}{2} \cdot \left(\frac{x}{L}\right)^2 + \frac{c}{3} \cdot \left(\frac{x}{L}\right)^3 \tag{4}$$

Our choice for the two nondimensionalized position coordinates should be done intentionally. Since expressions like $\frac{x}{L}$ show up so frequently, we'll choose to normalize the two

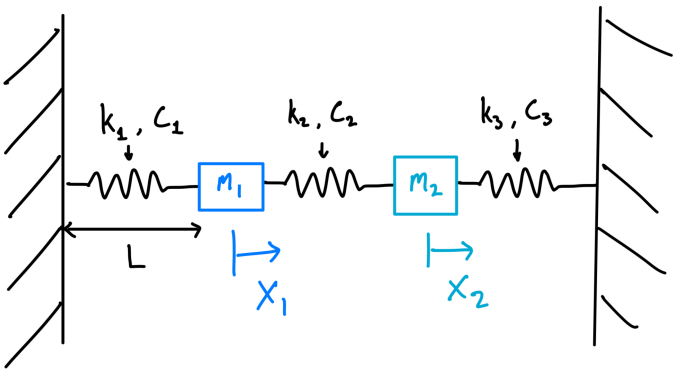


Figure 2: Our system is three non-linear springs in series, each with rest length $L$ and unique coefficients $k_i$ and $c_i$. Between adjacent springs are two masses, $m_1$ and $m_2$. Our coordinates $x_1, x_2$ are displacements from the equilibrium positions of the masses $m_1$ and $m_2$ respectively.

displacements from the rest length by $L$ to get:

$$q_1 = \frac{x_1}{L}, \quad q_2 = \frac{x_2}{L}$$

In order to write down a Lagrangian, we also need kinetic energy, which is defined simply for the one dimensional system as $T_i = \frac{1}{2}m_i x_i^2 = \frac{1}{2}m_i L^2 q_i^2$. So now we have all the pieces to write down our Lagrangian.

$$\begin{aligned}\mathscr{L} = &\frac{1}{2}m_1 L^2 \dot{q_1}^2 + \frac{1}{2}m_2 L^2 \dot{q_2}^2 - \\ &- \left(k_1 \frac{q_1^2}{2} + c_1 \frac{q_1^3}{3}\right) \\ &- \left(k_2 \frac{(q_2 - q_1)^2}{2} + c_2 \frac{(q_2 - q_1)^3}{3}\right) \\ &- \left(k_3 \frac{q_2^2}{2} + c_3 \frac{q_2^3}{3}\right)\end{aligned} \tag{5}$$

## 2.2 Non-dimensionalization and Euler-Lagrange Equations

We aim to non-dimensionalize this system, defining dimensionless variables for $x_1, x_2$, and $t$.

Focus first on $t$ –define a characteristic time scale to be $T$ with units time, such that $\tau = \frac{t}{T}$ is unitless. For our purposes, it is difficult to define one characteristic timescale for the behavior of the three springs, so the rest of this derivation is done assuming one such $T$ can be found. We chose parameters $m_i$ and $k_i$ to be the same order of magnitude such that the time-scale for simple harmonic motion $\sqrt{\frac{m}{k}} = T \approx 1$.

Look next to $x_1$ and $x_2$. A typical length scale will be of order the spring's rest length, defined as $L$, such that we have already non-dimensionalized each translational variable to be

$$q_1 = \frac{x_1}{L}, q_2 = \frac{x_2}{L}. \tag{6}$$

Time derivatives will now look like:

$$\frac{d}{dt} = \frac{d}{d\tau}\frac{d\tau}{dt} = \frac{1}{T}\frac{d}{d\tau} \tag{7}$$

and spatial derivatives will now look like:

$$\frac{d}{dx_i} = \frac{d}{dq_i}\frac{dq_i}{dx_i} = \frac{1}{L}\frac{d}{dq_i}, \text{ for } i \in [1, 2], \tag{8}$$

such that the Euler-Lagrange equations can be written as

$$\frac{1}{TL}\frac{d}{d\tau}(\frac{d\mathscr{L}}{d\dot{q_i}}) = \frac{d\mathscr{L}}{dq_i}. \tag{9}$$

The Lagrangian itself has already been non-dimensionalized as per these coordinate choices in 5. Apply 9 to achieve

$$\begin{aligned} \frac{1}{T}\frac{d}{d\tau}(m_1 L^2 \dot{q_1})^2 &= -k_1 q_1 - c_1 q_1^2 + k_2(q_2 - q_1) + c_2(q_2 - q_1)^2 \\ \ddot{q_1} &= \frac{T}{m_1 L^2}[-k_1 q_1 - c_1 q_1^2 + k_2(q_2 - q_1) + c_2(q_2 - q_1)^2], \end{aligned} \tag{10}$$

for the $\hat{q_1}$ Euler-Lagrange equation. Do the same for $\hat{q_2}$ to obtain

$$\begin{aligned} \frac{1}{T}\frac{d}{d\tau}(m_2 L^2 \dot{q_2})^2 &= -k_3 q_2 - c_3 q_2^2 - k_2(q_2 - q_1) - c_2(q_2 - q_1)^2 \\ \ddot{q_2} &= \frac{T}{m_2 L^2}[-k_3 q_2 - c_3 q_2^2 - k_2(q_2 - q_1) - c_2(q_2 - q_1)]. \end{aligned} \tag{11}$$

Note these are both dimensionless. We continue to solve these equations numerically.

## 3 Results

Throughout the following analysis, we use the following set of default system parameters unless otherwise mentioned or varied:

$$\begin{aligned} &m_1 = 1,\ m_2 = 1 \\ &k_1 = 3,\ k_2 = 3,\ k_3 = 3 \\ &c_1 = 1.5,\ c_2 = 1.5,\ c_3 = 1.5 \\ &T = 1,\ L = 1 \\ &\text{ICs: } q_1 = -0.5,\ q_2 = 0.5,\ \dot{q_1} = \dot{q_2} = 0 \end{aligned} \tag{12}$$

### 3.1 Classical Regime and Normal Modes

We reproduce the classical, non-chaotic system analog by setting the quadratic spring constants to zero, allowing us to analyze normal modes using linear algebra techniques as described in class. The following figures are using these parameters: $c_i = 0, k_i = 1, m_1 = m_2 = 1$ and these initial conditions: $q_1 = q_0 = 0$, $\dot{q}_1 = 0$, $\dot{q}_2 = -\frac{1}{2}$.

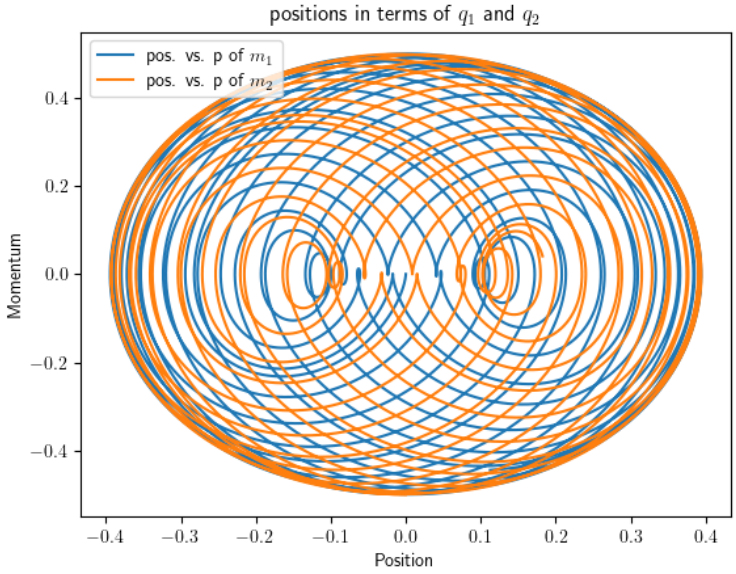


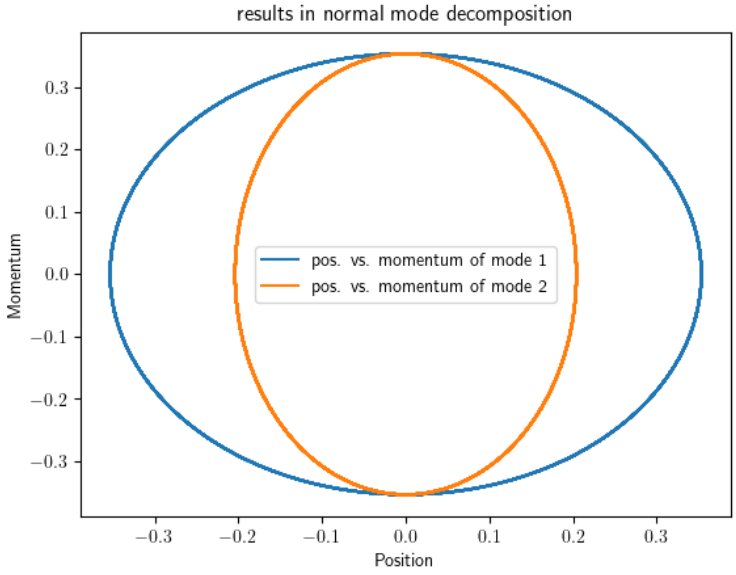

### 3.2 Dynamics with Varying Mass

Here, we keep the left mass $m_1$ constant while varying the right mass $m_2$. With a set initial condition for each case, we then analyzed the differences in motion between cases. Recall that if the quadratic spring constants were set to zero, this initial condition would result in predictable dynamics, as the springs would be in exactly one normal mode. This behavior, without quadratic terms, is demonstrated in Figure 3.

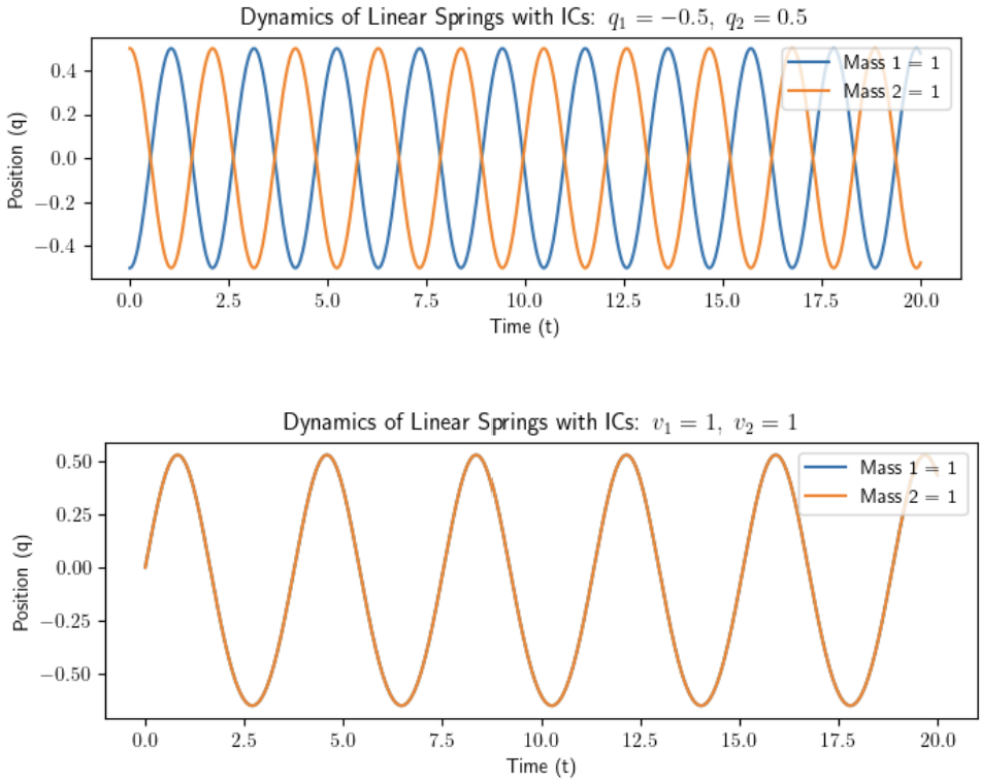


Figure 3: We provide two examples of normal-mode like behavior. The first situation has equal masses released at rest from equal and opposite displacements. This situation results in equal amplitude and period for each mass, albeit offset by a $\pi$ phase. The second situation has equal masses starting at their respective equilibrium positions ($q_1 = q_2 = 0$) and with velocity $\dot{q_1} = \dot{q_2} = 1$, resulting in equal amplitude and period with no phase difference.

We present initial conditions of the left mass at $q_1 = -0.5$ and the second mass at $q = 0.5$ non-dimensionalized units, in figure 4.

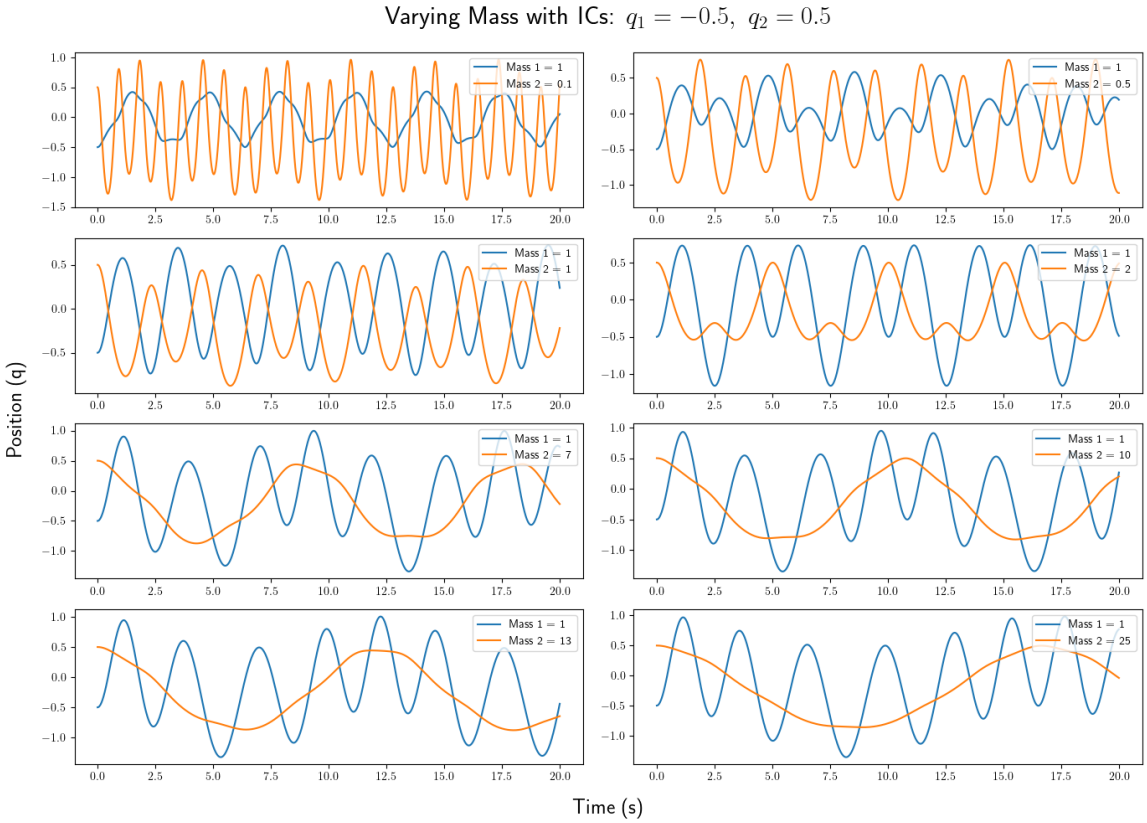


Figure 4: We vary mass, beginning with a lower mass difference at the top and larger difference at bottom of the figure. We observe non-linear fluctuations in the expected trend of $m_2$'s period decreasing as it becomes larger relative to $m_1$. Note particularly the $m_1 = m_2 = 1$ case, where we would expect with linear springs exactly offset sinusoids with non-varying amplitude, as in Figure 3. However, non-linearity produces this interesting behavior in the two mass system.

### 3.3 Dynamics with Varying Spring Constant

Here, we vary the linear and quadratic spring constants in two regimes: equal mass and non-equal mass.

Figure 5 demonstrates the equal mass case, where $m_1 = m_2 = 1$. As one moves from top to bottom, position vs. time plots show the period of oscillation decreasing, mapping closely to the intuition that stronger springs lead to a reduced period. We see amplitude stay constant throughout, and little chaotic behavior. However, as the quadratic spring constant increases, we begin to observe non-linear behavior.

Figure 6 demonstrates the non-equal mass case, where $m_1 = 0.5, m_2 = 1$, representing a scenario where the first mass is half of the mass of the second. We use identical initial conditions to the equal mass case, and compare the results. Each figure is discussed individ-

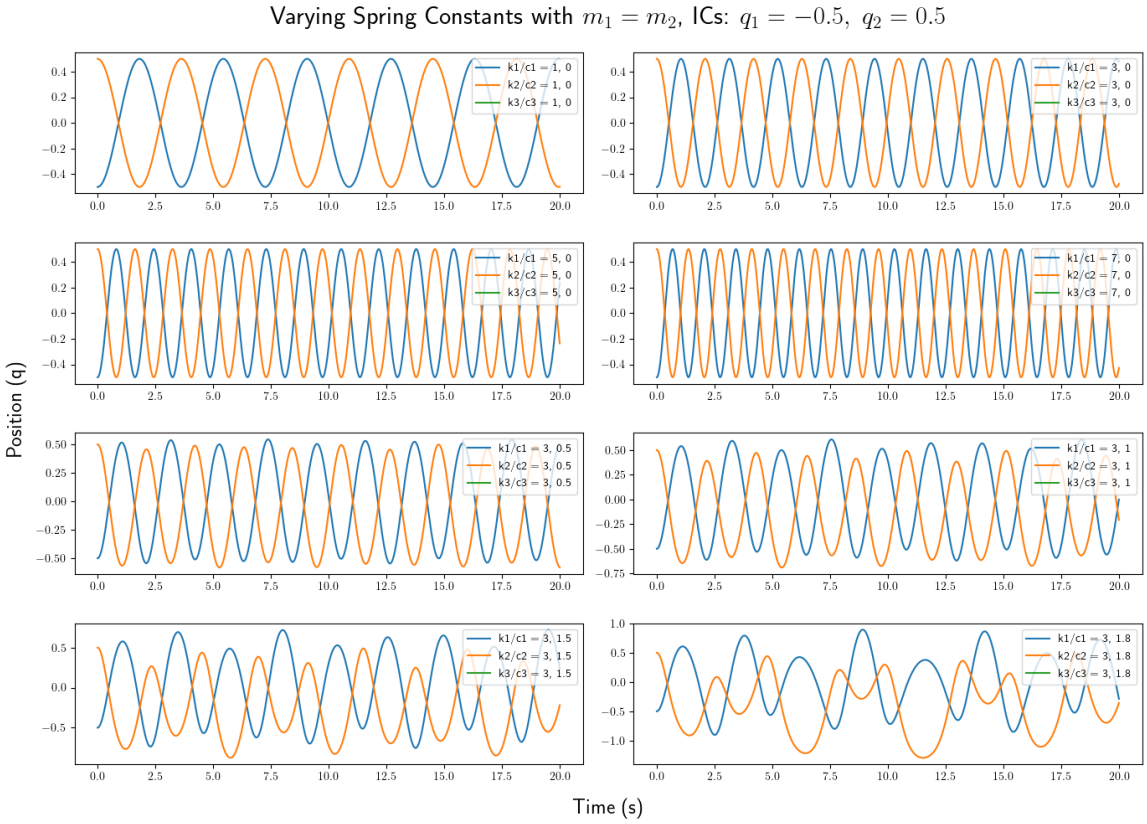


Figure 5: We vary spring constants, keeping $m_1 = m_2 = 1$ throughout. The upper four plots maintain a zero quadratic spring coefficient, and demonstrate the expected behavior of the period shrinking as the springs become stronger. The lower four plots keep the linear spring constants equal at $k_1 = k_2 = k_3 = 3$ while increasing the quadratic spring constant from 0.5 to 1.8, where we observe numerical instability if any $c_i > 1.8$.

ually in its caption. An important discovery from comparing the two cases is that there are regimes in which the spring non-linearity has less of an effect on overall dynamics. While in figure 5 we see a drastic change in period and amplitude between the quadratic spring constant $c = 0.5$ case to the $c = 1.8$ case, figure 6 shows less of a change, with only slight differences in phase.

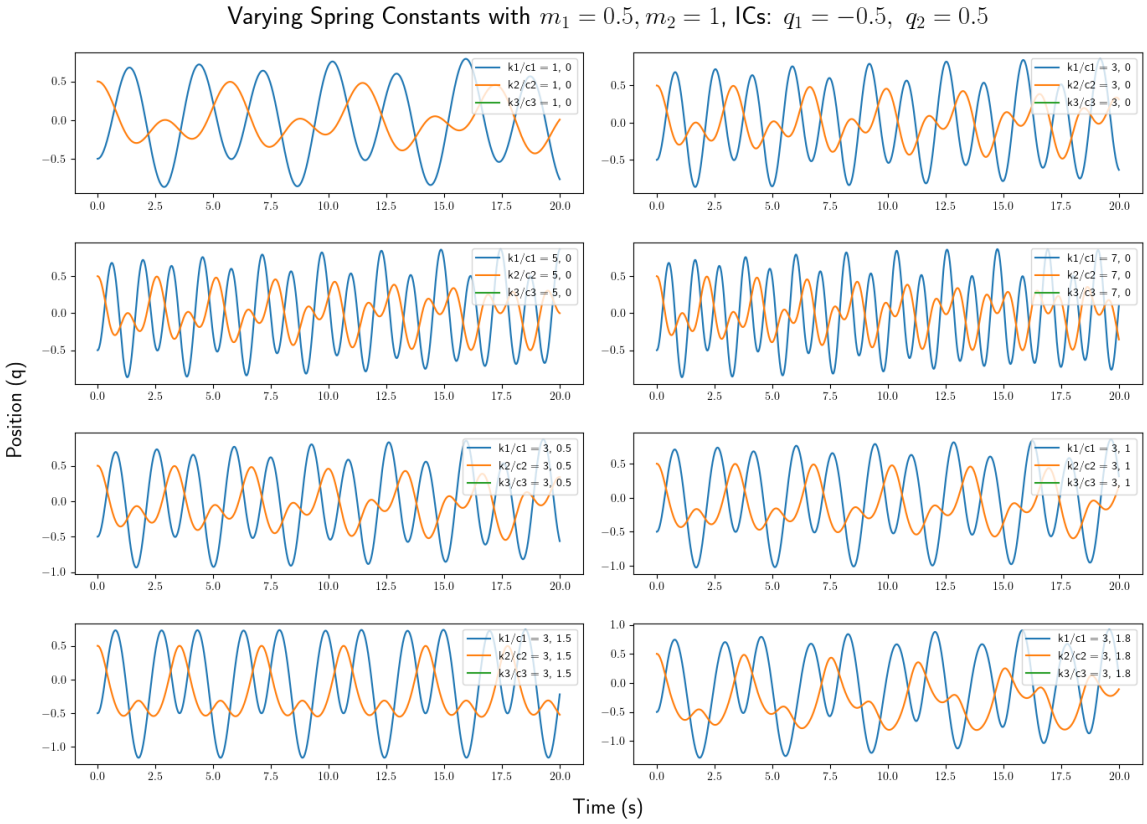


Figure 6: We vary spring constants while now having a 1:2 mass ratio, with $m_1 = 0.5, m_2 = 1$. An observation is that the dynamics are not changing nearly as much (in terms of shape) while the quadratic spring constants change. More specifically, the general peak shape and height are roughly constant in the bottom half of the graph, when they are non-zero and increasing.

### 3.4 Surface of Section

We demonstrate plots in phase space for each mass as the other mass is passing through its defined zero, also known as a surface of section. In figures 7 and 8, we keep the masses and spring constants constant, varying only initial conditions.

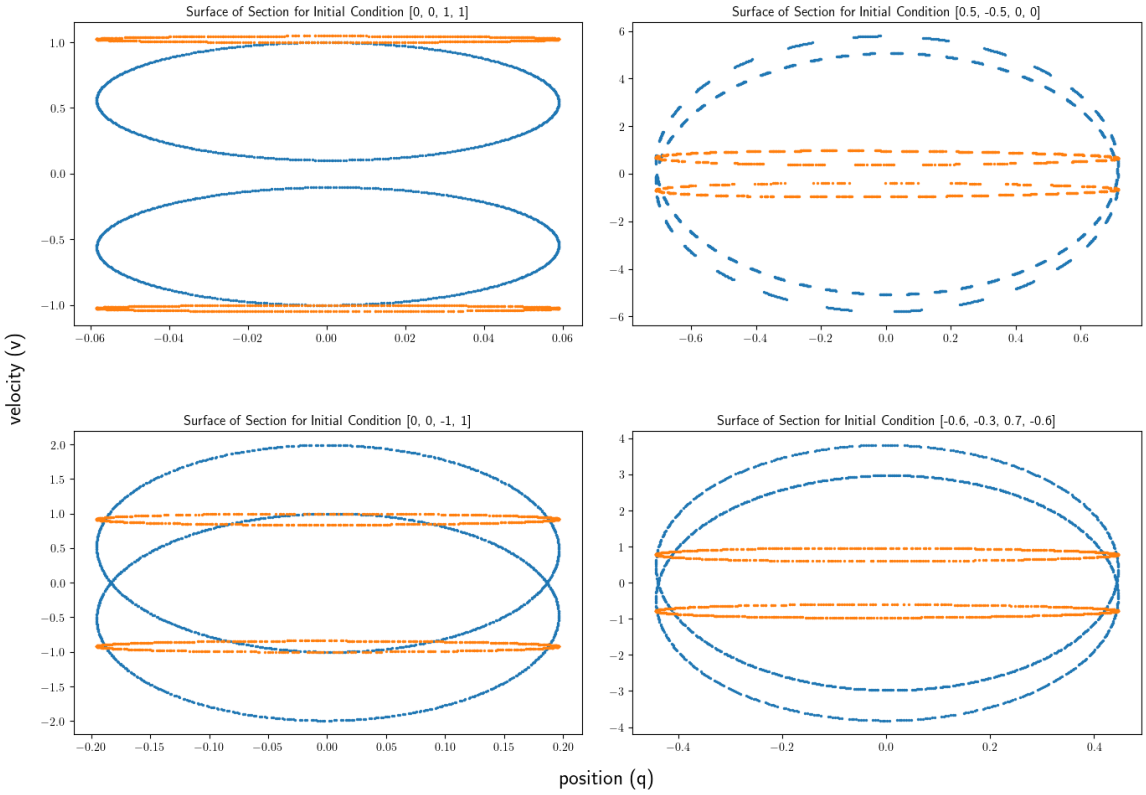


Figure 7: We first show surfaces of section for various initial conditions, with $m_1 = 0.1, m_2 = 1$. Each surface shows a closed loop; the $m_1$ loops while $q_2 = 0$ are thin, implying that $m_1$ has roughly constant velocity at $\pm 1$ whenever it has small mass compared to $m_2$. However, the $m_2$ loops do vary, showing that initial conditions have a greater impact on the large mass dynamics than the small mass dynamics.

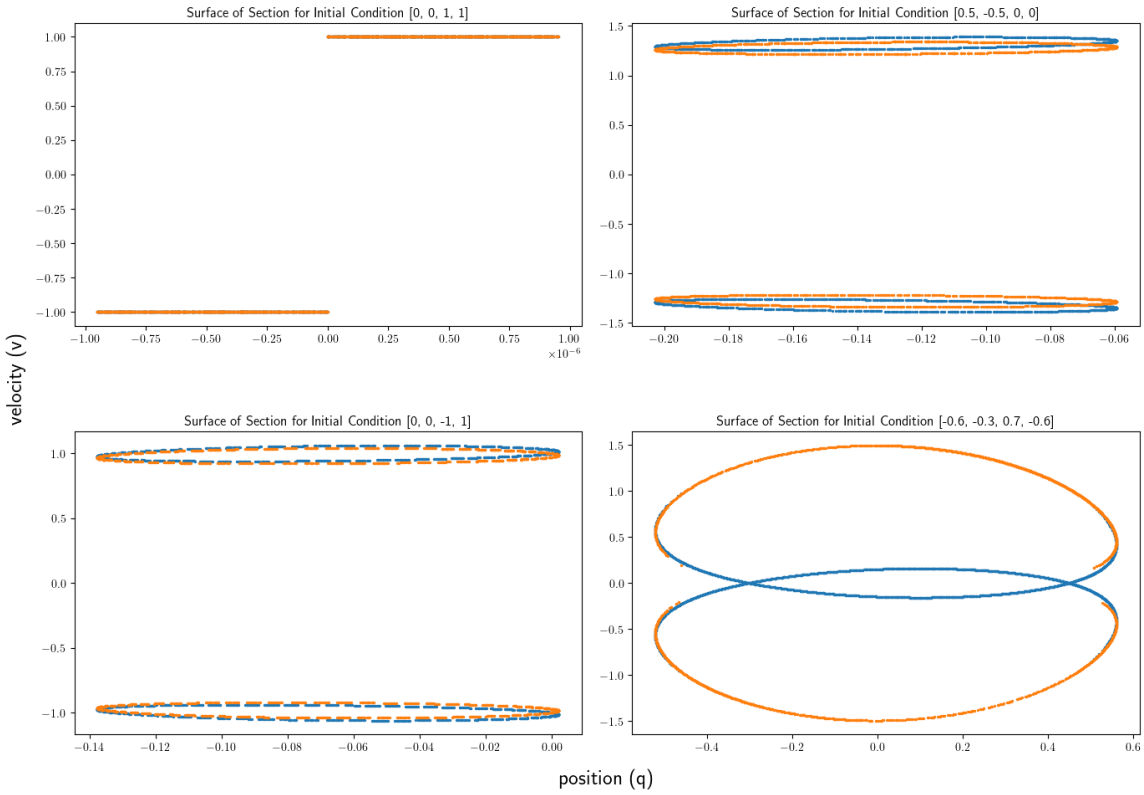


Figure 8: We create surfaces of section for various initial conditions, with $m_1 = m_2 = 1$. Each surface shows a closed loop. Interesting behavior occurs when each mass has velocity $\dot{q_1} = \dot{q_2} = 1$ and position 0, as the velocity is seen as instantaneously going from $-1$ to 1 and vice versa as in the top left plot. Further, more random initial conditions give rise to interesting motion as in the bottom right, where velocities and positions do fluctuate more readily.

# 4 Conclusion

As an entry point for studying stiffening biomaterials, we looked at the behavior of quadratic springs in series. To that end, we recovered the linear case (normal springs), experimented with varying the relataive masses, and varied the relationship between the three springs' linear and quadratic spring constants. To show the chaotic nature of the system, we generated qualitatively different surfaces of section for several sets of initial conditions. Please refer to our Jupyter notebook where we did most of the work.